Molecular-dynamics simulation of molecular-beam epitaxial growth of the silicon (100) surface

E. T. Gawlinski and J. D. Gunton
Physics Department and Center for Advanced Computational Science, Temple University, Philadelphia, Pennsylvania 19122
(Received 29 December 1986; revised manuscript received 6 May 1987)

We have simulated the growth of a Si(100) surface by deposition of silicon atoms from a molecular beam. A molecular-dynamics technique is employed where the equations of motion of 256 bulk particles and up to 256 additional adsorbed surface particles are solved exactly. We have used the Stillinger-Weber two- and three-body interaction potential to compute the forces between silicon atoms. Temperature and surface-reconstruction effects on the growth rate and surface morphology are studied. Bulk samples of Si are prepared at two temperatures, $T_{\text{low}}=\frac{1}{8}T_{\text{melt}}$ and $T_{\text{high}}=\frac{2}{3}T_{\text{melt}}$, and after a period of equilibration the beam is directed at the (100) surface. Prior to the deposition of new silicon and after the truncated bulk has come into equilibrium, the 2×1 dimer reconstruction is seen to have occurred. We observe the growth of an amorphous overlayer and the persistence of surface reconstruction at T_{low}. For the T_{high} case the growth is characterized by the formation of more ordered epilayers and the disappearance of the 2×1 surface reconstruction. These results are in qualitative agreement with experimental studies of the molecular-beam epitaxial (MBE) growth of the Si(100) surface.

I. INTRODUCTION

The study of crystal growth is one of the most important and productive areas of research in condensed matter, statistical, and solid-state physics. Aside from acting as an arena for research in such widely diverse areas ranging from phase transitions, nucleation kinetics, and domain growth in statistical physics to surface reconstruction, defects, and band theory in solid-state physics, it also has afforded enormous technological advantages. Modern crystal-growth techniques have revolutionized the computer and electronics industries. In the last decade alone, the ability to grow multilayer and multimaterial crystal structures has fostered major advances in the fabrication of electronic and optical devices.[1]

In this paper we present the results of a molecular dynamics study of molecular-beam-epitaxial growth of the Si(100) surface. One of our goals is to gain a better understanding of the role of surface-reconstruction phase transitions in the kinetics of nonequilibrium crystal growth. We are particularly interested in studying the role of substrate temperature in determining the morphology of the grown silicon overlayer, in particular, whether the growth results in amorphous or crystalline silicon.

MBE is a powerful and flexible technique for growing crystals. However, there are still a number of aspects of the growth process that are poorly understood. This is mostly due to the fact that crystal growth of this nature is a far-from-equilibrium phenomenon. There have been many experimental[1] and theoretical[2] attempts to address these questions but they have been of somewhat limited success. There has been very little computer simulation of the MBE problem,[3] however. Other crystal growth techniques such as growth from the melt and solution have been simulated mostly by Monte Carlo and molecular-dynamics methods.[4] Prior to the work described here, the only molecular-dynamics simulation of an MBE system was performed by Schneider *et al.*[5] in which they studied an idealized Lennard-Jones system. Their results indicate that epitaxial growth of well-ordered layers proceeds at all temperatures, but below a certain cutoff temperature T_s, the layers contain defects and voids. As we shall see below, our results for silicon grown by MBE differ in this regard and are more consistent with experimental results that indicate an epitaxial transition temperature. In fact, our work described herein was partially motivated by the experiment of Gossmann and Feldman[6] in which they monitored by high-energy ion scattering and channeling and low-energy electron diffraction the overlayer structure of silicon grown by MBE on its (100) surface. They studied this system at a variety of temperatures and found that below a certain temperature, usually called the epitaxial temperature, an amorphous growth structure results, whereas above this temperature growth proceeds in such a way as to yield well-ordered, layered structures. We undertook this simulation having in mind this effect and chose our growth temperatures such that they straddled the Gossmann-Feldman epitaxial temperature T_E, but were sufficiently higher and lower to account for any experimental uncertainty in the value of T_E.

Our long-term goals in simulating the MBE growth process are to understand the effects on the quality and morphology of the epilayers due to changes in various controllable parameters and uncontrollable aspects of the substrate. Examples of controllable parameters are the beam intensity and the substrate temperature. Uncontrollable aspects include surface reconstruction,[7] stress, and strain on the overlayer structure and surface diffusion. Unfortunately, the simulation of MBE using

molecular dynamics is an extremely computationally intensive undertaking. This paper reports some of our preliminary findings of a study designed primarily to aid in understanding of the effects of different substrate temperatures on the morphology of the grown overlayers. In some ways this simulation was a "proof of concept" and was partly done to explore the feasibility of doing computer simulations of such systems and to identify any potential problems. Simulations of this nature are also useful because they test the validity of the underlying interaction potentials used to describe the system. However, one could justifiably ask how extrapolations can be made from the results of a simulation based on the validity of a phenomenological potential. We address this question with the philosophy that the simulation results are useful as a component of a "feedback loop" involving experiment, theory, and simulation in which the interpretation of the results of any one stage is motivated in a self-consistent way by the remaining pair.

II. DETAILS OF THE SIMULATION

An Nth-order Gear predictor-corrector[8] integration algorithm was employed to integrate the equations. The first N derivatives of the position are calculated at time $t+\Delta t$ by Taylor-series expansions in terms of the same N derivative at time t;

$$\frac{d^n}{dt^n}\mathbf{r}^{(P)}(t+\Delta t)=\sum_{k=0}^{5-n}\frac{(\Delta t)^k}{k!}\frac{d^k}{dt^k}\mathbf{r}(t)\ , \qquad \forall n=0,1,\ldots,5\ . \tag{1}$$

The superscript (P) on the position vector indicates that this is the new *predicted* position. This new position is now corrected in the following way: The forces are reevaluated at the new predicted coordinates and compared with the forces determined from the new predicted accelerations. From the difference between these two estimates of the force, a force correction parameter is computed, viz.,

$$\Delta F=\tfrac{1}{2}(\Delta t)^2\left[\frac{1}{M}\mathbf{F}(t+\Delta t)-\frac{d^2}{dt^2}\mathbf{r}^{(P)}(t+\Delta t)\right], \tag{2}$$

where M, the single-particle mass, is taken equal to unity in our dimensionless units. The predicted parameters computed in Eq. (1) are now corrected with the Gear coefficients G_i^8 as follows:

$$\frac{d^n}{dt^n}\mathbf{r}^{(C)}(t+\Delta t)=\frac{d^n}{dt^n}\mathbf{r}^{(P)}(t+\Delta t)+\frac{n!}{(\Delta t)^n}G_n\Delta F \qquad \forall n=0,\ldots,5 \tag{3}$$

$$G_0=\tfrac{3}{20},\quad G_1=\tfrac{251}{360},\quad G_2=1,\quad G_3=\tfrac{11}{18},\quad G_u=\tfrac{1}{6}\ ,\quad \text{and}\quad G_5=\tfrac{1}{60}\ .$$

The superscript (C) denotes the corrected positions. These new corrected values are now taken as the current position, velocity, acceleration, etc., and all analyses at this time step are performed using these values. This entire procedure is then iterated for the duration of the simulation.

The interatomic potential that we chose to use in this simulation of silicon is due to Stillinger and Weber.[9] This potential involves both a two- and three-body term,

$$\Phi=\sum_{\substack{i,j\\ i<j}}v_2(i,j)+\sum_{\substack{i,j,k\\ (i<j<k)}}v_3(i,j,k)+\cdots\ , \tag{4}$$

where i, j, and k are particle labels and

$$v_2(r_{ij})=\varepsilon f_2(r_{ij}/\sigma)\ ,$$
$$v_3(\mathbf{r}_i,\mathbf{r}_j,\mathbf{r}_n)=\varepsilon f_3(|\mathbf{r}_i-\mathbf{r}_j|/\sigma,|\mathbf{r}_j-\mathbf{r}_k|/\sigma,|\mathbf{r}_k-\mathbf{r}_i|/\sigma). \tag{5}$$

Here ε is chosen to give f_2 a depth of -1 and σ is chosen to make $f_2(2^{1/2})$ vanish. This being done, all lengths and energies are hereafter dimensionless. The explicit form of the pair potential as a function of this dimensionless coordinate is

$$f_2(r)=\begin{cases}A(Br^{-p}-r^{-q})\exp[(r-a)^{-1}], & r<a\\ 0, & r\geq a\end{cases} \tag{6}$$

where A, B, p, and a are all positive. This function and all of its derivative are continuous at the cutoff $r=a$. The three-body interaction is composed of three terms,

$$f_3(|\mathbf{r}_i-\mathbf{r}_j|/\sigma,|\mathbf{r}_j-\mathbf{r}_k|/\sigma,|\mathbf{r}_k-\mathbf{r}_i|/\sigma)=h(r_{ij},r_{jk},\theta_{ijk}) \tag{7}$$

plus the cyclic permutations of i, j, and k, where θ_{jik} is the angle between the particles j and k subtended by particle i and r_{ij} is the distance between particles i and j (see Fig. 1). The function h has the form

$$h(r_{ij},r_{jk},\theta_{ijk})=\begin{cases}\lambda\exp[\gamma(r_{ij}-a)^{-1}+\gamma(r_{jk}-a)^{-1}](\cos\theta_{ijk}+\frac{1}{3})^2 & \text{for } r_{ij}<a \text{ and } r_{jk}<a\\ 0 \quad \text{otherwise}\ ,\end{cases} \tag{8}$$

where both λ and γ are greater than zero and the function and all its derivative are continuous at the cutoff at $r=a$. The ideal tetrahedral angle appropriate for the silicon crystal structure is favored by the $(\cos\theta_{jik}+\frac{1}{3})^2$ term.

Stillinger and Weber[9] have carried out a limited search over the seven parameters A, B, p, q, a, λ, and γ to find a reasonable set of values that reproduced the lattice sums (i.e., the cohesive energy) and melting point for real silicon. Their most satisfactory parameter set thus found is

$$A=7.049\,555\,627\,7,\quad B=0.602\,224\,558\,4,\quad p=4\ ,$$
$$q=0,\quad a=1.8,\quad \lambda=21.0,\quad \gamma=1.2\ . \tag{9}$$

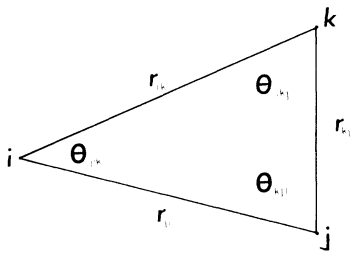

FIG. 1. Relevant parameters involved in the Stillinger-Weber potential. The indices i, j, and k label the individual silicon atoms. The r's are interparticle separations and the θ's are the angles defined by the triplets.

We have not tried to improve upon these values for our molecular beam epitaxy simulation. Late in the course of our work we also became aware of another silicon potential developed by Biswas and Hamann.[10] This potential takes into consideration both bulk and surface properties of silicon and therefore should, in principle, be more appropriate for our growth study. One of our next goals in silicon simulation is to redo part of the present study using the Biswas-Hamann potential.

Our simulation begins with the preparation of a truncated Si(100) surface that is allowed to come into equilibrium at either one of two temperatures, $T_{\text{high}}=0.06$ and $T_{\text{low}}=0.01$, measured in dimensionless units relative to the depth of the pair potential. The melting temperature in these units is approximately $T_{\text{melt}}=0.08$ as determined by Stillinger and Weber[9] and reconfirmed by us. We chose these two temperatures because they straddle the experimentally determined epitaxial transition temperature seen by Gossmann and Feldman,[6] $T_E\sim 0.034$, above which well formed epitaxial overlayers are grown and below which rather disordered amorphous overlayers form.

This surface layer is the eighth and topmost layer in a bulk silicon configuration with the [100] direction pointing in the positive z direction. Each layer consists of 32 silicon atoms and hence the original system contains 256 particles. Periodic boundary conditions apply in the x and y directions, whereas the topmost layer (substrate layer) has free boundary conditions, as does the bottom (first) layer. The latter is, however, subject to a viscous damping force that couples to the z component of the velocity of any particle in this layer. No attempt is made to obey the fluctuation-dissipation theorem with this artificial viscous force: It is not meant to simulate a heat bath but is present only to damp out any phonon modes that may be stimulated by the impinging molecular beam and would otherwise reflect off of a fixed boundary.

This original system forms a perfect diamond cubic lattice with lattice constant chosen such that the density is that of real silicon at room temperature, i.e., $\rho=0.4600$ in dimensionless units. Each silicon atom in this bulk substrate is given a velocity sampled from a Maxwellian distribution corresponding to the desired temperature and randomly directed. The equations of motion of each atom are then solved for 10 000 time steps where each time step is taken to be $\Delta t=0.01$, again in dimensionless units. This corresponds to a real time of 766 attoseconds. This period of equilibration was found sufficient for the system to minimize its total energy at both the higher and low temperature, thus attaining $E_{\min}(T_{\text{low}})=-1.77$ and $E_{\min}(T_{\text{high}})=-1.63$.

In Figs. 2(a) and 2(b) the topmost silicon (100) layer is shown both prior to and after the 10 000-step equilibration period at $T_{\text{high}}=0.06$. Figure 2(a) represents the (100) surface pattern as it would be found in the bulk, whereas Fig. 2(b) clearly shows the interesting 2×1 surface reconstruction that that Si(100) surface is known experimentally to display. (See Sec. III below for a discussion of this reconstruction and for relevant references.) One goal of this simulation is to study the effects of this reconstruction on the morphology of any overlayers sub-

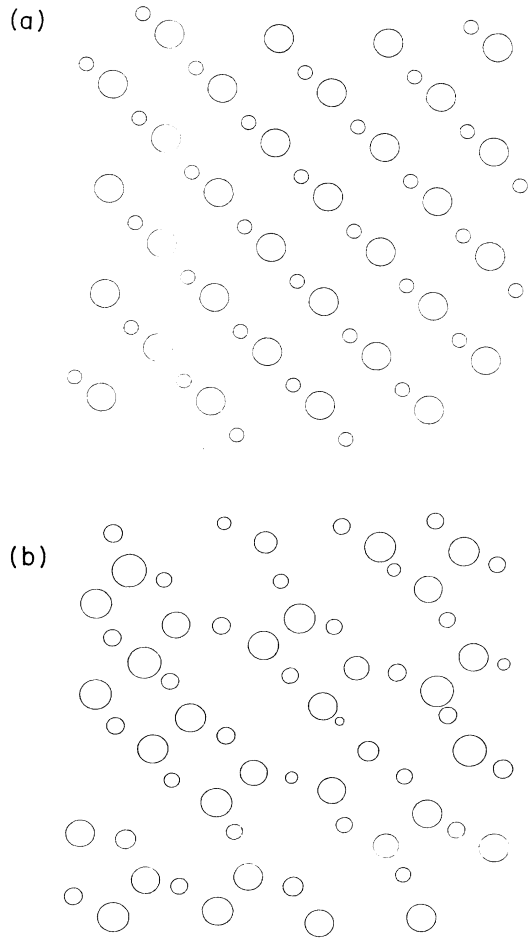

FIG. 2. (a) and (b): the Si(100) surface prior to and after the $10\,000\Delta t$ equilibration period at $T_{\text{high}}=0.06$ respectively. The large circles indicate the positions of the silicon atoms in the topmost (100) layer and the smaller circles represent those atoms in the next lower (100) layer. Shaded circles belong to dimer pairs that form the 2×1 reconstruction. Note that about 50% of the atoms in the topmost layer belong to dimer pairs.

sequently grown upon this surface as a function of temperature.

We now turn to a discussion of the simulation of our molecular beam and its interaction with the target substrate. One input parameter into our program is the number of layers we wish to grow. From this our program determines the z coordinates of an imaginary plane perpendicular to the [100] direction sufficiently far enough above the substrate surface that all the desired growth layers can be accommodated. This plane is used as the starting point for the silicon beam particles. Another input parameter is the frequency of particle deposition. Given this frequency, the creation of a beam particle can be triggered by the current time step of the simulation. This is accomplished by first choosing a random point in the imaginary plane mentioned above, creating a silicon atom at this point, and then assigning it a velocity $\mathbf{v}=-\sqrt{3T}\,\hat{\mathbf{z}}$, where T is the temperature of the bulk substrate and $\hat{\mathbf{z}}$ is the unit vector in the z direction. The beam temperature is taken equal to that of the bulk to simplify the thermalization of beam particles after their incidence upon the surface. The equations of motion of both beam and bulk particles are solved simultaneously with the only difference being that the beam particle velocities are not rescaled along with the bulk particle velocities when maintaining constant temperature. The fact that the Stillinger-Weber potential has a well defined cutoff provides a handy definition of when a particle belongs to the beam or to the bulk: A particle is said to leave the beam and join the bulk when it interacts with another bulk particle. After this point it is subject to the velocity rescaling done to maintain a constant bulk temperature. This is, in fact, how the beam particle gets thermalized after its collision with the silicon surface. One limitation that this process has is that the beam velocity becomes irrelevant; the interaction is so weak near the cutoff $r=a$ that the particle velocity gets rescaled long before any significant momentum can be transferred to the surface. This is a point we will address in a more realistic simulation to be done in the future, thereby permitting a study of the effects of the beam temperature on growth and morphology.

After allowing the bulk substrate to come into equilibrium by running for $10\,000\Delta t$, we switch on the beam and release a particle into it every $50\Delta t$ for the run at T_{high} and every $75\Delta t$ for the run at T_{low}. In both cases we grew an additional eight layers; that is, we deposited an additional 256 atoms, thus taking $12\,800\Delta t$ and $19\,200\Delta t$ for the high and low temperature runs respectively. The frequency of deposition at the low temperature was lower than that of the high temperature in order to reduce the number of interactions between beam atoms prior to their arrival at the surface. Subsequent to the growth stage, we annealed both the high- and low-temperature configurations for an additional $50\,000\Delta t$ each. The entire simulation therefore entailed a total of 152 000 time steps. Significant additional computer time was spent in testing and refining the procedure. In all, approximately 500 h of Cyber 205 and FPS 264 CPU time were used in the simulation.

In Sec. III we present the results of our simulation and, when relevant, discuss its relation to both experiment and theory.

III. RESULTS

In Figs. 2(a) and 2(b) we show the (100) surface of the bulk silicon upon which the molecular beam will be incident. Figure 2(a) depicts the surface immediately after truncation of the bulk, whereas Fig. 2(b) shows the same surface after the $10\,000\Delta t$ equilibration period at $T_{\text{high}}=0.06$. The large circles in this figure are meant to represent the 32 silicon atoms in the topmost layer and the smaller circles are those of the next layer down in the bulk. The circle sizes are inversely proportional to their distance from the viewer. The outstanding feature seen in Fig. 2(b) is the "dimerization" of silicon atoms sitting in adjacent rows. A dimer is the bonding of two neighboring atoms due to the rehybridization of the surface dangling bonds. Pairs of silicon atoms belonging to the same dimer are shown shaded.

There is now ample theoretical and experimental evidence that surface atoms having two dangling bonds (as in the case of the silicon (100) surface) form a dimer to lower their energy and collectively lead to a 2×1 reconstructed surface. However, there is still some controversy over the structural details of the dimers.[11] One such detail is the asymmetry of the dimer with respect to the (100) plane: It is now widely believed that the dimer pairs are *not* parallel to the (100) surface but rather are tilted into this plane. Evidence indicating this has been gathered using a variety of techniques such as medium-energy ion scattering, low-energy electron diffraction, helium diffraction and photoemission. In addition, there have been theoretical predictions indicating asymmetry by employing both pseudopotential calculations and energy minimization using the semiempirical tight-binding approximation.[12]

In our simulation we see that, indeed, dimers form on the (100) surface. However, there is no evidence of any asymmetry. This is not surprising in light of some of the proposed mechanisms for forming asymmetric dimer pairs: The energy-minimization calculations predict a charge transfer between the silicon atoms leading to a more energetically favorable tilted configuration. The Stillinger-Weber potential makes no provision for any such electronic transition, and, in fact, it is rather remarkable that a potential purely based upon bulk structural and thermodynamic properties leads to any dimerization at all.

Nor have we seen any temperature effects to the degree that the amount of dimerization observed in our simulation is about the same for both T_{high} and T_{low}. At either temperature about 50% of the surface silicon atoms belong to a dimer pair, as is evident in Fig. 2. We do not, however, observe a perfect 2×1 reconstruction but rather small 2×1 domains separated by antiphase boundaries. This phenomenon is also seen in the scattering experiments on the Si(100) surface as indicated by the broadening of the 2×1 spots in the diffraction pattern. Presumably this configuration is a long-lived metastable state,

however we are uncertain as to what extent the finite size of our system would effect the lifetime of such a state.

In Figs. 3(a) and 3(b) we have plotted the density of the silicon system as a function of the z coordinate, that is, the density along the growth axis. Figure 3(a) corresponds to the system depicted in Fig. 2(a) and similarly for Figs. 2(b) and 3(b). In Fig. 3(a) we see eight peaks of equal height corresponding to the eight layers of 32 silicon atoms in our initial state. We see, on the other hand, in Fig. 3(b) the density as it appears for the system after its $10\,000\Delta t$ equilibration period. The new features in this plot are the broadening and shortening of the peak in the topmost (reconstructed) layer and the overall nonmonoticity of the height of the peaks as a function of increasing z. This last effect is presumably due to subsurface relaxation induced by the strain caused by the reconstruction. The data presented in Figs. 2(b) and 3(b) are for the T_{high} run. These same plots made for the T_{low} run are qualitatively the same. However, the density profile has somewhat sharper peaks.

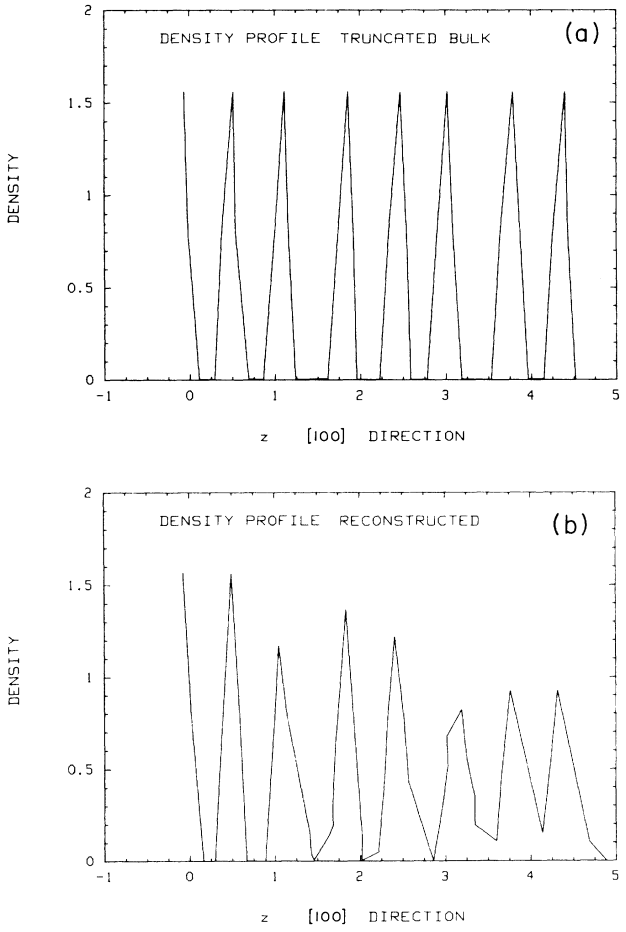

FIG. 3. Density profiles parallel to the [100] direction for the configurations shown shown in Figs. 2(a) and 2(b). (a) shows the uniform density profile of a perfectly ordered bulk held at $T=0.0$. (b) on the other hand, indicates the nonzero temperature by a broadening of the peaks. The interesting nonmonotonic decay of the peak heights as the surface is approached from the bulk is perhaps due to the relaxation of subsurface strain induced by the 2×1 reconstruction seen in (b).

As mentioned above the growth process was simulated by periodically creating a new silicon atom in an imaginary plane parallel to the (100) surface and at a height above the surface sufficient to accommodate the growth of an additional number of layers (eight layers in this case). Each new particle's x and y coordinates were chosen randomly and the particle was given a downward velocity corresponding to the average velocity of the atoms in the bulk. The frequency of creation of new particles was chosen to reduce the chance of beam atoms interacting with one another during their traversal to the surface. As described in detail in Sec. II, the simulation was carried out for $12\,800\Delta t$ and $19\,200\Delta t$ for T_{high} and T_{low}, respectively, yielding 256 new bulk particles sufficient for an additional eight new layers.

Because of the excessive amount of computer time necessary to perform a molecular-dynamics (MD) simulation of this system we have been unable to deposit enough particles to get into a steady-state growth mode. Furthermore, the deposition rate is excessively high in comparison with real MBE experiments. We feel, therefore, that it is perhaps unsafe to draw any conclusions about the *dynamical* aspects of this growth and hence restrict ourselves to a study of the effects of the substrate temperature and reconstruction upon the *morphology* of the deposited overlayers. To this end, we have annealed both the high- and low-temperature runs for $50\,000\Delta t$ after the deposition of the additional 256 silicon atoms.

Cross sectional views parallel to the (100) surface for T_{low} and T_{high} are shown in Figs. 4 and 5, respectively. Each subfigure shows a *pair* of layers similar to Fig. 2. Figures 4(b) and 5(b) show the seventh and the eighth layers denoted by small and large circles respectively; recall that layer eight was the original substrate for the adsorbed atoms. Figures 4(a) and 4(b) are views of layers five through eight of the original bulk silicon and Figs. 4(c) and 4(d) are layers nine through twelve and were grown by deposition from the beam. The slices through the grown part of the system were made at points where the pairs of layers would lie if the bulk pattern had been continued up to that point. The convention that the smaller the circle the more distant it is from the viewer is maintained only within one subfigure. Effectively, Figs. 4 and 5 depict a cross-sectional view of the resultant system *as one passes through the interface between the substrate and the grown epilayers.*

Examining Fig. 4(b) we see that even after annealing the system for $50\,000\Delta t$ the surface reconstruction is still prevalent to the degree it was prior to growth. Figures 4(c) and 4(d) indicate that there is very little order within the layers parallel to the (100) plane. We shall see in Fig. 6(a) that, in fact, there is no detectable ordering in the z direction either. Therefore, the result of the growth at T_{low} is a very poorly ordered, or perhaps even amorphous, slab of silicon. On the other hand, Fig. 5, which displays the T_{high} data, shows both a destruction of the 2×1 reconstruction in the original substrate sur-

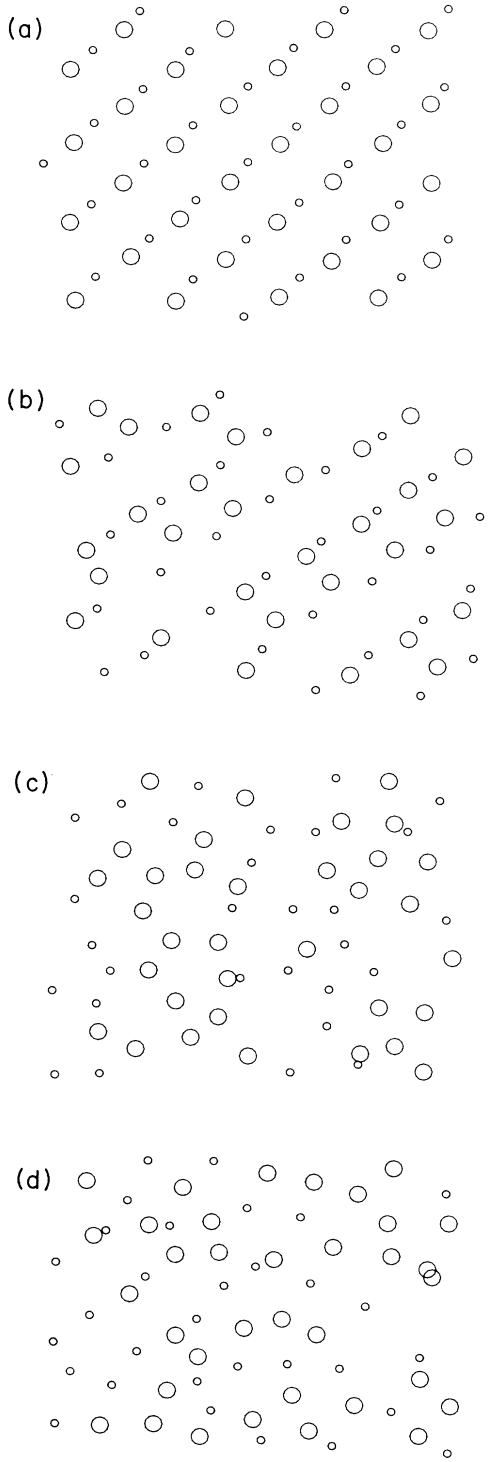

FIG. 4. Cross-sectional view of the interface after growth and annealing at $T_{low}=0.01$. Each subfigure shows a pair of layers similar to Fig. 2. (a) and (b) depict layers five through six and seven through eight, respectively. Layer eight [large circles in (b)] was the original (100) layer that the molecular beam was incident upon. Layers nine through twelve depicted in (c) and (d) are those that were grown from the beam. Note the persistence of the reconstruction in (b) and the lack of order in the overlayers.

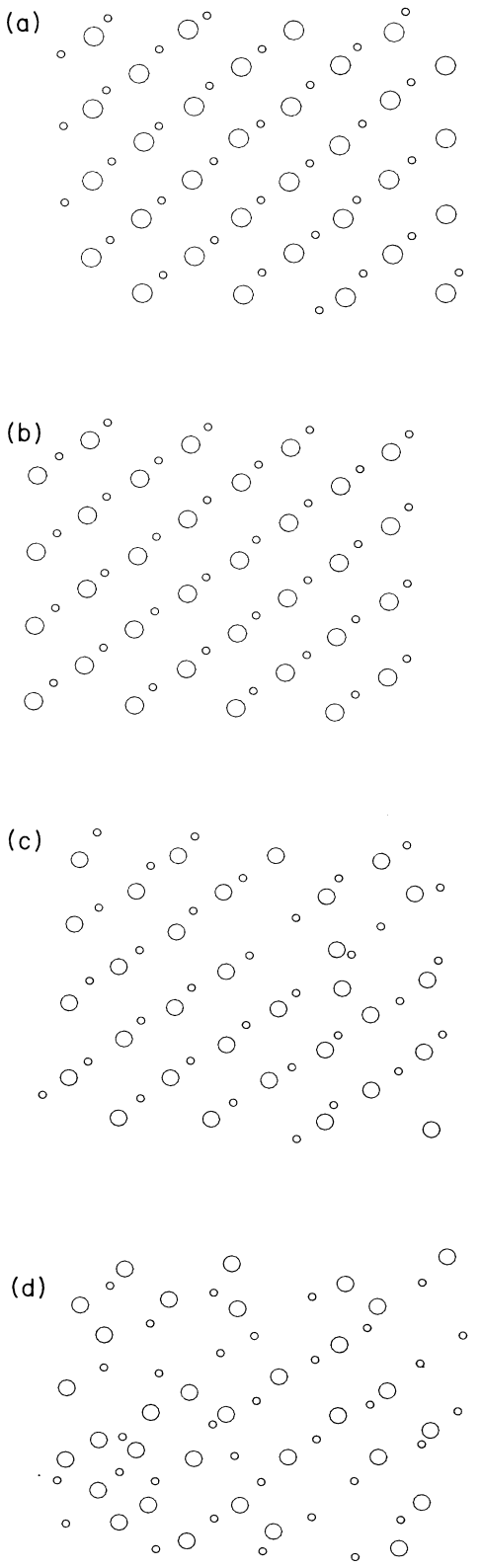

FIG. 5. Same as Fig. 4 but at $T_{high}=0.06$. Note the absence of reconstruction in (b) and the well ordered overlayers in Fig. (c).

face [Fig. 5(b), i.e., layer eight], and a much more ordered intralayer structure, at least in the first three grown layers [Figs. 5(c) and 5(d)].

The density profiles along the z direction [i.e., the density within (100) slices] are shown in Figs. 6(a) and 6(b) for T_{low} and T_{high}, respectively. As mentioned above, the profile for the T_{low} run shows almost no structure with the exception of a small and broad peak just above the original substrate surface. In the case of T_{high}, however, the layering of the grown silicon is very evident. Figure 6(b) shows, quite clearly, an additional three or possibly four well-defined layers. It is important to note that the diminished peak two layers below the original substrate surface is still present in the T_{low} run, even after annealing for $50\,000\Delta t$. This is the same feature that was present in the density profiles for initial bulk (see Fig. 3) and is presumably attributable to the persistence of the 2×1 reconstruction at T_{low}; *persistent even in the presence of the grown amorphous overlayer.*

These results are consistent with the results of Gossmann and Feldman[8] who, by using both low energy electron diffraction (LEED) and high-energy ion scattering and channeling, have shown that at 300 K ($T=0.018$ in our dimensionless units) the growth of overlayers deposited by MBE on the Si(100) surface are highly imperfect. They have studied the MBE growth of the Si(100) surface over a range of temperatures and found that only above a temperature approximately equal to 570 K, the so called epitaxial temperature, are well defined epilayers formed. In our units, 570 K corresponds to $T\sim0.034$ and is therefore about halfway between T_{low} and T_{high}. Gossmann and Feldman do, however, observe that even below the epitaxial temperature the 2×1 reconstruction is reordered to its original bulk pattern. This reordering occurs down to the lowest temperature that they studied, that being 300 K or $T=0.018$. This temperature is not too much higher than our T_{low} but the difference could account for our seeing persistence of the 2×1 reconstruction in our simulation. A more likely explanation of this disagreement is that because of the very short real time that our simulation spans, even including the $50\,000\Delta t$ annealing period, our system is still in a state that is very far from equilibrium. If we were able to extend our simulation out to 10^6 or even $10^7\Delta t$, then we might observe reordering. As well, of course, the Stillinger-Weber potential may not be an adequate enough representation of the microscopic interactions between silicon atoms at a surface to predict this phenomena.

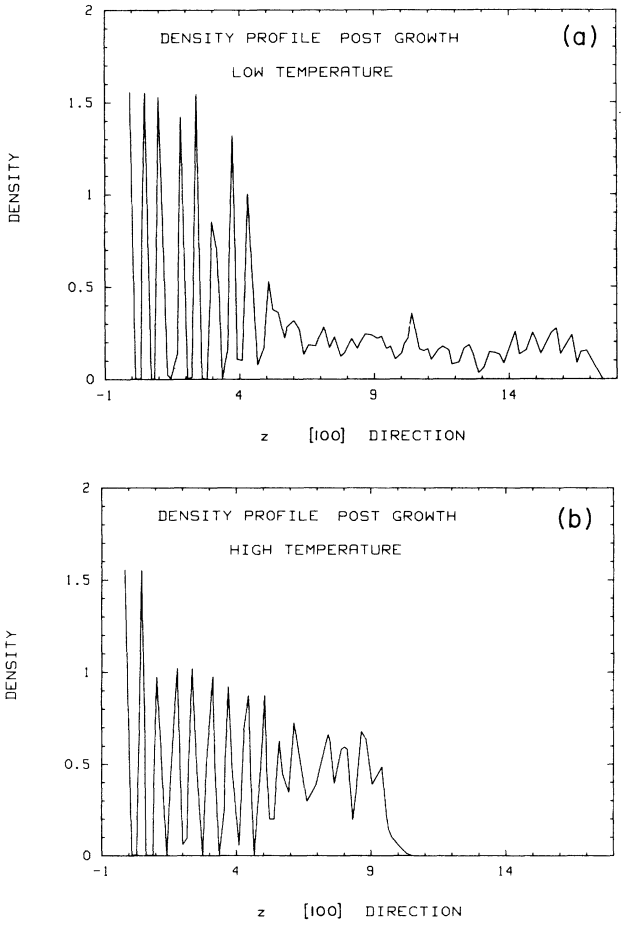

FIG. 6. Density profiles in the [100] direction of the configuration depicted in Figs. 4 and 5 are shown here in (a) and (b), respectively. Contrast the distinct peaks present in the growth profiles at the high temperature with the high-density amorphous overlayer grown at low temperature.

IV. CONCLUSIONS

In this paper we have shown that molecular dynamics is a viable simulation technique for studying the molecular beam epitaxial growth of semiconductor surfaces. The advantages of using MD are directly attributable to the ability to study, *in situ*, the microscopic, gross structural and thermodynamic properties of the system as a function of time. The limitations of the technique are due to the necessity of using phenomenological potentials in solving the equations of motion of the individual atoms. In the case of semiconductor surfaces, the most serious problem of this nature is the lack of consideration of the electronic degrees of freedom in these potentials. The band structure, electronic rehybridization and its consequential surface reconstruction, and other electronic properties are excluded. Another serious limitation is the amount of computer resources necessary even to attempt a modest simulation such as the one described here.

These difficulties notwithstanding, we have been able to make detailed inferences from our simulation, the most important of which is the verification of an epitaxial transition. Such a transition has been seen experimentally in the Si(100) MBE growth by Gossmann and Feldman[6] at $T_E\sim570$ K ($T=0.034$ in our dimensionless units). It is interesting to note that in the simulation of Schneider *et al.*,[5] where they studied the MBE growth of a Lennard-Jones system by molecular dynamics, no evidence of an epitaxial transition was found. For all temperatures studied the authors find layered growth. However, below a transition temperature T_s they find that the

layers are corrupted by dislocations, defects, and voids.

Further simulation is necessary to estimate the actual epitaxial temperature, and the details of the dynamics of MBE growth would have to be carefully studied in order to ascertain the nature of the temperature dependence. It would be interesting to test the conjecture that the breaking of dimer bonds is a simple activated process. Another interesting question to be addressed is the surface diffusion of silicon atoms on the clean 2×1 reconstructed (100) surface. Perhaps because of the dangling bonds being tied up in dimer pairs and the consequent reduction of covalent bonds formed with the substrate atoms, the surface silicon atoms may have a higher mobility.

With more realistic potentials and better computer facilities we should be able, with MD simulation, to shed light on these questions and others and better understand the MBE growth process.

ACKNOWLEDGMENTS

We would like to acknowledge useful discussions with Professor Martin Grant, Professor Jorge Viñals, and Professor Kimmo Kaski. We would also like to thank Dr. Enrico Clementi for his hospitality at IBM Kingston and for the use of the IBM 1CAP parallel processing system. Part of this research was conducted on the Cyber 205 at Colorado State University under National Science Foundation Grant No. DMR-8612609 and by a grant from the National Science Foundation Office of Advanced Scientific Computing. This research was also supported by the Office of Naval Research through Grant No. N00014-83-K-0382. We also acknowledge The Institute for Computational Studies at the Colorado State University at Fort Collins and all the support staff there that helped with the porting of the program to the Cyber 205.

[1]S. S. Lau and J. W. Mayer, *Treatise on Material Science and Technology* (Academic, New York, 1982), Vol. 24, Chap. 3; C. E. C. Wood, *Physics of Thin Films,* (Academic, New York, 1980), Vol. 2, p. 35; J. C. Bean, in *Impurity Doping,* edited by F. Wang (North-Holland, Amsterdam, 1981), Chap. 4; E. Kasper, Appl. Phys. A **28**, 129 (1982).

[2]J. A. Venables, G. D. T. Spiller, and M. Hanbucken, Rep. Prog. Phys. **47**, 399 (1984); J. D. Weeks and G. H. Gilmer, Adv. Chem. Phys. **40**, 157 (1979); S. V. Ghaisas and A. Madhukar, Phys. Rev. Lett. **56**, 1066 (1986); J. Singh and K. K. Bajaj, J. Vac. Sci. Technol. B **2**, 576 (1984); G. Gilmer, Science **208**, 355 (1980).

[3]J. Singh and A. Madhukar, J. Vac. Sci. Technol. B **1**, 305 (1983); C. Ebner, C. Rottman, and M. Wortis, Phys. Rev. B **28**, 4186 (1983).

[4]U. Landman, C. L. Cleveland, and C. S. Brown, in *Ordering in Two Dimensions,* edited by S. Sinha (Elsevier/North-Holland, Amsterdam, 1980), p. 335; J. Broughton and G. Gilmer, J. Chem. Phys. **79**, 5095 (1983); **79**, 5105 (1983); **79**, 5119 (1983); J. Q. Broughton, A. Broissent, and F. Abraham, *ibid.* **74**, 4029 (1981); Y. Hiwatari, E. Stoll, and T. Schneider, *ibid.* **68**, 3401 (1978); F. Abraham and G. M. White, J. Appl. Phys. **41**, 1841 (1970); D. Nicholson and N. G. Parsonage, *Computer Simulation and the Statistical Mechanics of Adsorption* (Academic, New York, 1982); F. Abraham, J. Vac. Sci. Technol. B **2**, 534 (1984); Adv. Phys. **35**, 1 (1986); F. Abraham and G. Broughton, Phys. Rev. Lett. **56**, 734 (1986).

[5]M. Schneider, A. Rahaman, and I. K. Schuller, Phys. Rev. Lett. **55**, 604 (1985).

[6]H. J. Gossmann and L. C. Feldman, Phys. Rev. B **32**, 6 (1985).

[7]L. J. Giling and W. J. P. van Enckevort, Surf. Sci. **161**, 567 (1980).

[8]C. W. Gear, *Numerical Initial Value Problems in Ordinary Differential Equations* (Prentice Hall, Englewood Cliffs, 1971).

[9]F. Stillinger and T. Weber, Phys. Rev. B **31**, 5262 (1985).

[10]R. Biswas and D. R. Hamann, Phys. Rev. Lett. **55**, 2001 (1985).

[11]H. H. Farrel, F. Stucki, J. Anderson, D. J. Frankel, G. J. Lapeyre, and M. Levinson, Phys. Rev. B **30**, 721 (1984); W. S. Yang, F. Jona, and P. M. Marcus, Solid State Commun. **43**, 847 (1982); M. T. Yin and M. L. Cohen, Phys. Rev. B **24**, 2303 (1981).

[12]D. J. Chadi, Phys. Rev. Lett. **43**, 43 (1979); R. M. Tromp, R. G. Smeenk, F. W. Saris, and D. J. Chadi, Surf. Sci. **133**, 137 (1983); R. M. Tromp, R. G. Smeenk, and F. W. Saris, Phys. Rev. Lett. **46**, 939 (1981); Solid State Commun. **39**, 755 (1981); B. W. Holland, C. B. Duke, and A. Paton, Surf. Sci. **140**, L269 (1984); W. S. Verwoerd, Surf. Sci. **99**, 581 (1980); **129** (1983); M. T. Yin and M. L. Cohen, Phys. Rev. B **24**, 2303 (1981); A. Kahn, Surf. Sci. Rep. **3**, 193 (1983).